Biomedicine & Pharmacotherapy 188 (2025) 118166

Contents lists available at ScienceDirect

Biomedicine & Pharmacotherapy

journal homepage: www.elsevier.com/locate/biopha

Fenofibrate treatment during lactation prevents liver and adipose tissue associated metabolic dysfunction in a rat model of childhood obesity

Lucas Paulo Jacinto Saavedra [a,*], Scarlett Rodrigues Raposo [a], Ana Letícia Manso Assakawa [a], Naiara Cristina Lucredi [e], Maria Natália Chimirri Peres [a], Silvano Piovan [b], Gessica Dutra Gonçalves [a], Veridiana Mota Moreira [a], Letícia Ferreira Barbosa [a], Diana Sousa [d,g,h], Flávia Caroline Farias dos Santos [c], Andreia Amaro [d,g,h], Marcos Divino Ferreira-Junior [m], Jones Bernardes Graceli [c,n], Paulo Matafome [d], Jurandir Fernando Comar [e], Rodrigo Mello Gomes [f,i,j], Josep C. Jiménez-Chillarón [k,l], Douglas Lopes Almeida [b,*,1], Paulo Cezar de Freitas Mathias [a,*,1]

[a] Department of Biotechnology, Genetics, and Cellular Biology, State University of Maringá, Maringá, PR, Brazil
[b] Department of Biochemistry, State University of West Paraná, Cascavel, PR, Brazil
[c] Department of Morphology, Federal University of Espírito Santo, Vitória, Brazil
[d] Institute of Physiology and Institute of Clinical and Biomedical Research, Faculty of Medicine and Center for Innovative Biomedicine and Biotechnology, University of Coimbra, Coimbra, Portugal Coimbra Health School, ESTeSC, Instituto Politécnico de Coimbra, Coimbra, Portugal Clinical Academic Center of Coimbra, Coimbra, Portugal
[e] Department of Biochemistry, State University of Maringá, Maringá, PR, Brazil
[f] Laboratory of Endocrine Physiology and MetabolismDepartment of Physiological Sciences, Federal University of Goiás, Goiânia, GO, Brazil
[g] Institute of Pharmacology and Experimental Therapeutics, Faculty of Medicine, University of Coimbra, Azinhaga de Santa Comba, Coimbra 3000-548, Portugal
[h] CIBB—Centre for Innovative Biomedicine and Biotechnology, University of Coimbra. Institute of Pharmacology and Experimental Therapeutics, Faculty of Medicine. Ph. D. Programme in Experimental Biology and Biomedicine (PDBEB), Institute for Interdisciplinary Research (IIIUC), University of Coimbra, Azinhaga de Santa Comba, Coimbra 3000-548, Portugal
[i] Department of Structural and Functional Biology, Institute of Biology, Universidade Estadual de Campinas (UNICAMP), Campinas, São Paulo, Brazil
[j] Obesity and Comorbidities Research Center, Universidade Estadual de Campinas (UNICAMP), Campinas, SP, Brazil
[k] Institut de Recerca Sant Joan de Déu (IRSJD), Endocrinology, Esplugues, Spain
[l] Universitat de Barcelona-Facultat Medicina-Bellvitge, L'Hospitalet, Spain
[m] State University of Campinas, Brazil
[n] Animal Science, School of Agricultural Sciences, Southern Illinois University, Carbondale, IL, USA

ARTICLE INFO

Keywords:
Small litter
Childhood obesity
FGFR1
FGF21
PPAR-alpha

ABSTRACT

Childhood obesity and associated comorbidities in adulthood are of great concern worldwide. Evidence highlights the importance of lactation in later disease development. In this sense, obese children are at great risk of developing adult obesity, insulin resistance, type 2 diabetes, and cardiovascular disease at adulthood. PPARα activation during lactation promotes the expression of key enzymes involved in lipid oxidation, and it was associated with reduced adiposity in children. Therefore, we hypothesized that an animal model of childhood obesity, small litter (SL), would lead to the development of obesity and metabolic dysfunction in adulthood, which could be prevented by postnatal PPARα agonism. Wistar dams had their litter reduced, leading to postnatal overfeeding and obesity early in life. SL male pups were treated with fenofibrate, an PPARα agonist, during lactation, from postnatal day (PND) 1 until weaning (PND21), to verify whether PPARα activation prevents the developmental programming at adulthood (PND120). Childhood obesity induced by postnatal overfeeding leads to decreased markers for oxidative metabolism during infancy, leading to increased visceral adiposity and

Abbreviations: PND, Postnatal day; BAT, Brown adipose tissue; VAT, Visceral adipose tissue; SL, Small Litter; DAG, Diacylglicerol; HFD, High-fat diet.

* Correspondence to: Department of Biotechnology, Cell Biology 10 and Genetics, State University of Maringá 5790 Av Colombo, Sala 19, 11, Maringá, PR 87020-900, Brazil.
E-mail addresses: saavedralpj@gmail.com (L.P.J. Saavedra), pmathias@uem.br (P.C.F. Mathias).
[1] Both authors contributed equally

https://doi.org/10.1016/j.biopha.2025.118166
Received 12 March 2025; Received in revised form 8 May 2025; Accepted 9 May 2025
Available online 19 May 2025

oxidative stress, insulin resistance, hepatic microvesicular steatosis, and increased fibroblast growth factor 21 (*Fgf21*) expression, followed by decreased brown adipose tissue (BAT) sympathetic nerve activity and decreased *Fgfr1* hypothalamic expression in adulthood. Agonist-induced PPARα activation during lactation mitigated the development of aforementioned alterations in adulthood. Postnatal fenofibrate treatment prevents the developmental programming of visceral obesity, liver-associated metabolic dysfunction and BAT autonomic sympathetic hypoactivity in an animal model of childhood obesity.

1. Introduction

Childhood obesity is a condition of major health concern. In 1990 it was estimated that 2 % of children and adolescents were obese. In 2022 this value has tripled, reaching 8 % of children and adolescent population worldwide [1]. Childhood obesity is associated with increased risk for the onset of type 2 diabetes and cardiovascular disease, at adulthood [2–4]. Infancy and lactation are well-established "windows" for metabolic programming for disease at adulthood [5,6]. Epidemiological data have shown that six months exclusive breastfeeding is protective against the development of disease later in life [7]. Additional stimuli during lactation may confer protective effects against metabolic dysfunction induced during adulthood, such as maternal low-protein diet and exercise [8,9]. On the other hand, several experimental studies have shown that nutritional/environmental stresses in this critical phase of development, including maternal obesity, diabetes, increased glycation and smoking, overfeeding and formula intake may have long-term effects on the metabolism of offspring, promoting the development of obesity, cardiovascular disease and metabolic dysfunction during adulthood [10–12].

Postnatal overfeeding by litter size reduction (2–4 pups per mother) has become a valid experimental model for childhood obesity, leading to early life metabolic dysfunction and obesity which persists and aggravates later in life [13,14]. In fact, postnatal overfeeding is reported to cause liver steatosis, insulin resistance, cardiovascular dysfunction, dyslipidemia and dysregulation of glycemic homeostasis at adulthood [13,15,16]. The Peroxisome Proliferator Activated by Receptor – alpha (PPARα) has a major role in lipid oxidation since it is a transcriptional factor for the expression of key genes involved in lipid oxidation and ketogenesis [17]. During gestation, the fetus is nourished through the cord blood where glucose is the main energy source. After birth, the breastmilk, rich in lipids, is the primary source of nutrition to the neonate, characterizing a nutritional switch from carbohydrate to lipid metabolism [18]. Breastmilk derived free fatty acids activate PPARα into the neonate liver, promoting DNA demethylation and increasing transcription of genes involved in β-oxidation and lipid metabolism, such as *Cpt1a*, *Acox* and *Fgf21* [19]. In adult animals, activation of PPARα prevented obesity and ameliorated metabolic dysfunction induced by high fat-diet (HFD) [20].

Considering that obesity during infancy is (1) associated with the development of obesity and metabolic dysfunction at adulthood, and (2) that PPARα activation is an important event to promote lipid oxidation early in life, here we hypothesize that activating PPARα during lactation might prevent the development of obesity in a rat model of childhood obesity and late onset of metabolic dysfunction.

2. Methods

2.1. Animal handling and experimental design

Wistar rats, males and females, were obtained from the Maringá State University Central Animals Facility and housed in the Animal Facility of the Experimental Laboratory of DOHaD (LExDOHaD), kept under controlled condition of temperature (22 ± 2ºC), and photoperiod (12 hours dark-light cycle). Animals had ad libitum access to standard chow and water throughout the experimental period. Animals were mated in a ratio of 1 male for 2 females. All the animal handling, housing and experimental procedures followed the guidelines of the Brazilian National Council for Control of Animal Experimentation (CONCEA) and were approved by the Ethic Commission in The Use of Animals (CEUA) from State University of Maringá, Brazil (Protocol Number 8934110422).

2.1.1. Experiment 1 – Childhood obesity induced deleterious health outcomes are prevented by postnatal activation of PPARα

Birth was considered postnatal-day zero (PND0). At PND 1 all litters were standardized for nine pups per mother, with the surplus pups being euthanized, maintaining the proportion of five-to-six males and four-to-three females in each litter. Fenofibrate (F - Infinity Pharma, COD: 1454, LT: 20F15-B030–063706) was dissolved in 10 % DMSO (Sigma, D2650) and 15 % kolliphor HS 15 (Sigma, 42 966). At PND1 litters were randomly assigned to Vehicle (V - 15 % Koliphor and 10 %DMSO in distilled water) or Treated (F – 12.5 mg/kg in vehicle) by intraperitoneal injections from PND1 until weaning, PND21 [21]. At PND3 the number of pups was adjusted to three males per dam for small litters (SL), and kept 9 pups per dam in the normal litter (NL). The surplus pups from SL were euthanized. Forming the experimental groups with the following number of litters: NL-V (n = 10), SL-V (n = 10), NL-F (n = 10), and SL-F (n = 11) – Fig. 1. Considering the sexual dimorphism, since females do not develop marked insulin resistance and non-hepatic steatosis (NAFLD) when reared in SL [22], only males were used in this study for assessments during lactation and after weaning. After weaning PND21, animals were housed at three per cage until PND120, when experimental procedures were performed, namely, insulin tolerance, euthanasia for plasma and tissue collection, and sympathetic nerve electrical activity. Food intake and body weight (BW) gain were measured weekly during the experimental period. Visceral adiposity index was calculated as the sum of the three main visceral fat depots (retroperitoneal, perigonadal and mesenteric), in relationship to animal weight. Visceral Adiposity %= [(Retro + Perig + Mesent)/Bw] *100. β-hydroxybutyrate was randomly measured in capillary blood of pups, at PND7,14 and 21 using a glucometer and β-ketone test strips. (FreeStyle Optimum®, Abbot). We choose to show data from this experiment separately, first, NL-V against SL-V (Figs. 3, 4 and 6), then SL-V against SL-F (Figs. 7, 8 and 9), to facilitate data interpretation and to test our hypothesis: Increased PPARα activation early in life prevents the development of obesity and metabolic dysfunction programmed by childhood obesity.

2.1.2. Experiment 2 – Childhood obesity alters markers of oxidative metabolism early in life

Considering our hypothesis that the observed phenotype of obesity could be related to a decrease in oxidative metabolic pathways early in life, we choose to perform an experiment for those markers in organs important for energy balance control, namely, liver, adipose tissue and brown adipose tissue (BAT). Similarly, to Experiment 1, after birth, PND 0, litters were standardized for 9 pups per litter, and then, at PND3 randomly litters were assigned to NL or SL, litters from NL were kept for 9, and SL had their litters reduced to 3 pups per litter. Animals were euthanatized for tissue sample collection at PND14. Forming the experimental groups with the following number of litters: NL (n = 4), SL-V (n = 5). Afterwards samples were processed for western blotting for different antibodies (Supplemental Table 1). Animals had free access to food and water during the whole experiment.

2.2. Indirect calorimetry and sympathetic nerve activity

From each group, a random set of animals at PN119 were used for indirect calorimetry and nerve register. O2 consumption and CO2 production were assessed for 24 hours (Oxylet system; Pan Lab/Harvard Instruments, Barcelona, Spain). 24 hours energy expenditure (EE) and respiratory quotient (RQ) were then calculated using the O2 and CO2 data by Metabolism® Software (Pan Lab/Harvard Instruments) [23]. During the procedures rats had ad libitum access to food and water.

From each group, a random set of animals from different litters were subjected to measurement of sympathetic nerve activity. Animals were anesthetized using Sodium Thiopental (45 mg/kg of body weight) after overnight fasting (12 hours). The sympathetic nerve branch, which innervates the BAT, was surgically exposed and placed over a pair of platinum recording electrodes. Recordings were made with a Bio-Amplificator (Insight®, Ribeirão Preto, Brazil) in the 1–80 kHz range and amplified 10000-fold, as previously described [23]. The nerve activity was recorded for 10 min, and the average numbers of spikes/5 s were used to calculate the nerve firing rate from five to seven sections of 15 s recordings for each rat.

2.3. Insulin sensitivity, tissue collection and biochemical analysis

From each group, a random set of PND119 animals from different litters were subjected to intra-peritoneal insulin tolerance test (ipITT). Animals were fasted for 6 hours and glycemia was measured (0' time), then animals received an intraperitoneal injection of insulin (1U/kg – NovoRapid, NovoNordisk ®,), and the blood glucose was measured at 15', 30' and 60 minutes using a glucometer (FreeStyle Optimum®, Abbot) as previously described [24]. The plasma glucose disappearance rate was calculated (K_{itt}) by the formula $= 0.693/ t½$, where $t½$ is calculated from the slope of the plasma glucose concentration post-insulin injection until basal rates at 60 min after insulin injection, as previously described [25].

After 48 hours of recovery, following an overnight fasting, animals were euthanized by decapitation for tissue and blood sample collection. Blood was centrifuged (10000 RPM, 5 min), plasma was collected and stored at −20°C. Plasmatic concentrations of glucose, total cholesterol, and triglycerides were quantified by spectrophotometry in a microplate reader (Kasuaki®), using commercial kits by following manufacturer's instructions (Gold Analise®, Belo Horizonte/MG, Brazil). Samples from retroperitoneal, liver, BAT and hypothalamus were quickly frozen in liquid nitrogen and then stored in −80°C for total lipid and molecular biology analysis or fixed in 10 % formalin for histological procedures.

2.4. RNA isolation and real-time quantitative RT-qPCR

Liver and hypothalamus samples previously stored at −80°C had their RNA isolated using TRIzol™ (Invitrogen®) following manufacturer's instructions. Total RNA concentration was measured spectrophotometrically at 260 nm (NanoDrop ND 1000 NanoDrop Technologies, Wilmington, DE). Total RNA was used for reverse transcription followed by real-time quantitative PCR (RT-qPCR). For cDNA synthesis 2 μg of RNA was reverse transcribed by the GoScript Reverse Transcription System (Promega, Madison, USA), and the quantification of the tissue expression of selected genes (Supplementary information, Table 2) was done by quantitative PCR in a Corbett Rotor-Gene 6000® (Qiagen) with GoTaq® qPCR Master Mix (Promega). *β-actin* expression was used as housekeeping gene. The $2^{-\Delta CT}$ method was used for the relative quantification analysis and data were expressed in arbitrary units (AU) [26]. The sequence of primers used were described (Supplemental Table 2).

2.5. Western blotting

Tissue samples were homogenized in a RIPA lysis buffer (25 mM Tris/HCl pH 7.6, 150 mM NaCl, EDTA 5 mM, 1 % Triton x100, sodium deoxycholate 1 %, SDS 1 %, 1Mm PMSF, sodium orthovanadate 1 mM, pyrophosphate 2 mM, sodium fluoride 10 mM, EGTA 1 mM and Aprotinin 2 μg/mL) and centrifuged two times 12.000 ×g for 15 min. The pellet was discarded and the supernatant was used. Extracted sample total protein was determined according using Pierce™ BCA Protein Assay Kit (Thermofischer). Samples containing 20 μg protein were combined with Laemmli sample buffer (50 mM Tris–HCl pH 6.8, 10 % glycerol, 2 % SDS, 0.025 % bromophenol blue, 5 % β-mercaptoethanol), heated at 98°C for 5 minutes for protein denaturation, applied on 10 %

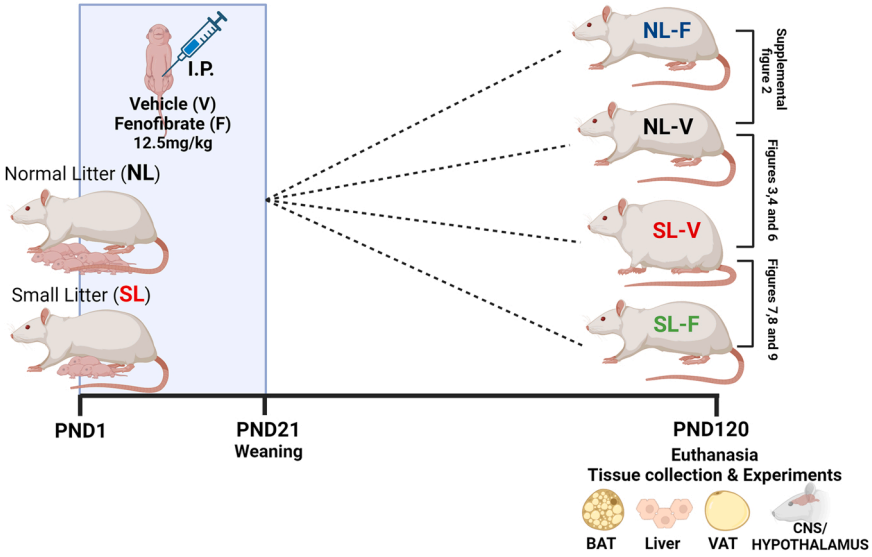

Fig. 1. Schematic representation of Experiment 1. From birth until weaning, pups from different litters received by intraperitoneal injections either Vehicle (V) or PPARα agonist, Fenofibrate 12.5 mg/kg (F). At postnatal day (PND) 3, to induce obesity, litters were standardized for Normal litter (NL – 9 pups) or Small litter (SL – 3 pups), therefore forming the NL-V, SL-V and SL-F groups. After weaning animals were had free access to food and water, until PND 120 when experiments were performed. To facilitate data interpretation, comparisons were performed between NL-V and SL-V, Figs. 3,4 and 6, to test the hypothesis that childhood obesity would lead to obesity and metabolic dysfunction at adulthood. And then SL-V was compared against SL-F, Figs. 7, 8 and 9, to test the hypothesis that postnatal increase activation of PPARα would protect against the development of obesity and metabolic dysfunction induced by childhood obesity. Created with BioRender.com.

SDS-PAGE (sodium dodecyl sulfate polyacrylamide gel electrophoresis), and transferred to PVDF membranes for one-hour 100 V. These membranes were blocked in a Tris-buffered saline (TBS-T - 10 mM Tris base, 150 mM NaCl and 0.25 % (v/v) of Tween 20) containing 5 % (w/v) non-fat dried milk for 1 h at room temperature. Afterwards, membranes were incubated overnight at 4°C with primary antibodies (anti-UCP1 - U6382, Sigma Aldrich; anti-β-actin, Santa Cruz Biotechnology cat. sc-47778), all of them were diluted 1:1000. Afterwards membranes were washed in TBS-T and incubated with a whole molecule peroxidase-conjugated secondary antibody (Anti-Goat, Sigma Aldrich, A5420, diluted 1:5000) for two hours and then washed in TBS-T. Band detection was performed by chemiluminescence (Amersham™ ECL Prime Western Blotting Detection Reagent, GE Healthcare, Chicago, IL, USA) and the bands were visualized using the ImageQuant LAS 500® (GE Healthcare Life Sciences, Chicago, IL, USA). Band intensities were analyzed using ImageJ software (National Institute of Health, Maryland, USA). Calnexin was used as a housekeeping protein.

2.6. Liver lipid extraction

Total lipid content in the liver was determined using the gravimetric method adapted from Folch et al. (1957) [27]. Briefly, liver samples (150 mg) were homogenized in a chloroform-methanol mixture (2:1). The result referring to the content of total lipids was expressed in percentage (g/100 g of wet liver weight). Liver triglycerides were determined by spectrophotometry in the total lipid extract, diluted in isopropyl alcohol, using commercial kit as previously described in the biochemical analysis section of this paper, results were expressed as mg/g of liver.

2.7. Histology

Liver, BAT and VAT (Visceral Adipose Tissue - retroperitoneal) tissues were fixed in formalin (10 % formaldehyde in PBS, pH 6.8) and embedded in paraffin to non-serial sections of 5 μm. Three non-serial sections per animal were placed in glass slides and stained in hematoxylin/eosin. The morphological study was performed utilizing digital images, randomly acquired (TIFF format, 36-bit color, 1360 ×1024 pixels) with a digital camera (CMOS 12.0 MP camera Bioptika) coupled to a light microscope (Axioscop, Zeiss). For VAT adipocyte diameter, the area of all adipocytes in 10 different pictures (x400 magnification) of the sections were measured by circulating adipocytes with free hand tool using ImageJ software (National Institute of Health, Maryland, USA), and calculating the total area of the adipocyte. For liver lipid inclusion analysis, 5 photos (x1000 magnification) of 3 different sections per animal was used. Microvesicular steatosis quantification was measured by point counting in a system consisting of 36 test points (Tp), where the density of microvesicular steatosis was (Vv) was estimated as the percentage of points hitting lipid inclusion vesicles (Pp), Vv [steatosis, liver] = Pp[steatosis]/Tp, as previously described [28,29]. For BAT percentual lipid area 10 photos (x1000 magnification) of 3 different sections per animal were used. Adapted from Piao et al., [30], images were converted to black and white using an image analysis software (Image J), then a threshold (Shanbhag) was applied, to highlight lipid vacuoles from lipids, and then the white area was measured, using the tool "particles analyze". The white area was divided from the total area of the picture, and the results presented as % of the area.

2.8. Oxidative stress

Liver and VAT tissue were collected to evaluate oxidative stress using thiobarbituric acid reactive substance assay (TBARS) and reduced glutathione (GSH) assays. Thus, Liver and white adipose tissue liver tissues were prepared for a GSH and TBARS reactive species quantification assay, measuring malondialdehyde (MDA, nmol/mg of protein) levels, as previously described [31,32].

2.9. Statistical analysis

Data analyze was performed using GraphPad-Prism® Software version 9.00 for Windows (GraphPad Software Inc., La Jolla California USA, www.graphpad.com). Results were presented as mean ± standard error of the mean (SEM). The data were analyzed through Student's *t*-test for parametric data and Mann-Whitney for non-parametric. Values of $p < 0.05$ were considered as the significance level. When Mann-Witney test was used, asterisk was represented in grey in the figure.

3. Results

3.1. Postnatal overfeeding leads to visceral obesity and metabolic dysfunction at adulthood

Early in life, SL-V animals have increased weight gain during lactation characterizing the model of childhood obesity (Fig. 2a), which persisted during post-weaning phase (Fig. 2b), leading to obesity at adulthood, PND 120 (Fig. 2b). Also, no difference on food intake was observed (Fig. 2c). At adulthood, obesity induced during childhood led to increased visceral obesity index (Fig. 2d), increased visceral adipocyte area (Fig. 2e), with increased retroperitoneal (Fig. 2f), perigonadal (Fig. 2g) and mesenteric (Fig. 2h) visceral fat depots. Obese animals had a trend for increased triglycerides (Fig. 2i, NL-V 102.8 *vs* SL-V 138 ± 11.66 mg/dL, $p = 0.07$). Finally, SL-V rats maintained normal glycemic levels (Fig. 2j), but developed insulin resistance (Fig. 2k, l, NL-V 1.06 ± 0.08 *vs* SL-V 0.77 ± 0.08 %/min, $p < 0.05$). No difference was observed on oxidative stress markers in adipose tissue (Supplemental Figure 1 – b, c). Considering the central role of liver in energy metabolism, and the metabolic dysfunction observed, we hypothesized that childhood obesity could program to hepatic steatosis.

3.2. Postnatal overfeeding leads to hepatic microvesicular steatosis, oxidative stress and increased FGF21 expression at adulthood

Childhood obesity did not modify liver weight (Fig. 3a) but led to increased steatosis at adulthood, as evidenced by liver histological analysis (Fig. 3b, NL-V 11.72 7 ± 1.756 *vs* SL-V 24.17 ± 0.914 %, $p < 0.001$), and triglycerides content (Fig. 3c, NL-V 75.95 ± 3.11 *vs* SL-V 99.13 ± 8.76 mg/g, $p < 0.05$). In agreement, the expression of *Fasn*, a key limiting enzyme on TAG synthesis, was elevated in the liver of obese rats, however no statistical difference was observed (Fig. 3d).

Furthermore, animals had increased MDA, indicating oxidative stress (Fig. 3e). Also, it was observed increased *Fgf21* expression in the liver (Fig. 3f, NL-V 0.896 ± 0.256 *vs* SL-V 4.242 ± .1174 A.U., $p < 0.05$) and no difference was observed on the expression of pro-inflammatory markers (Fig. 3 – g, h, i). Considering the observed phenotype of obesity and liver lipid accumulation, we hypothesized that litter size reduction, leads to decreased oxidative metabolism in organs involved in the regulation of energy homeostasis.

3.3. Postnatal overfeeding leads to decreased oxidative metabolism markers early in life (PND14)

We explored whether defects on hepatic oxidative metabolism were the consequence of progressive ageing-related metabolic derangement or was already altered during early life. Hence, animals were evaluated during lactation, at PND14. In the liver we observed decreased total AMPK (tAMPK - Fig. 4a), and phosphorylated AMPK (pAMPK – Fig. 4b). Since SL rats consumed more milk, that in turn contained higher concentration of lipids, it would be expected to result in an increase in oxidative metabolism in the liver [22]. At PND7, we observed increased serum β-hydroxybutyrate, which could be an indicative of increased hepatic oxidation of fatty acids (Figure Supplemental Figure 1a). However, no difference was observed at PND14 or PND21, which is in accordance to decreased pAMPK at PND14. Together, these data could

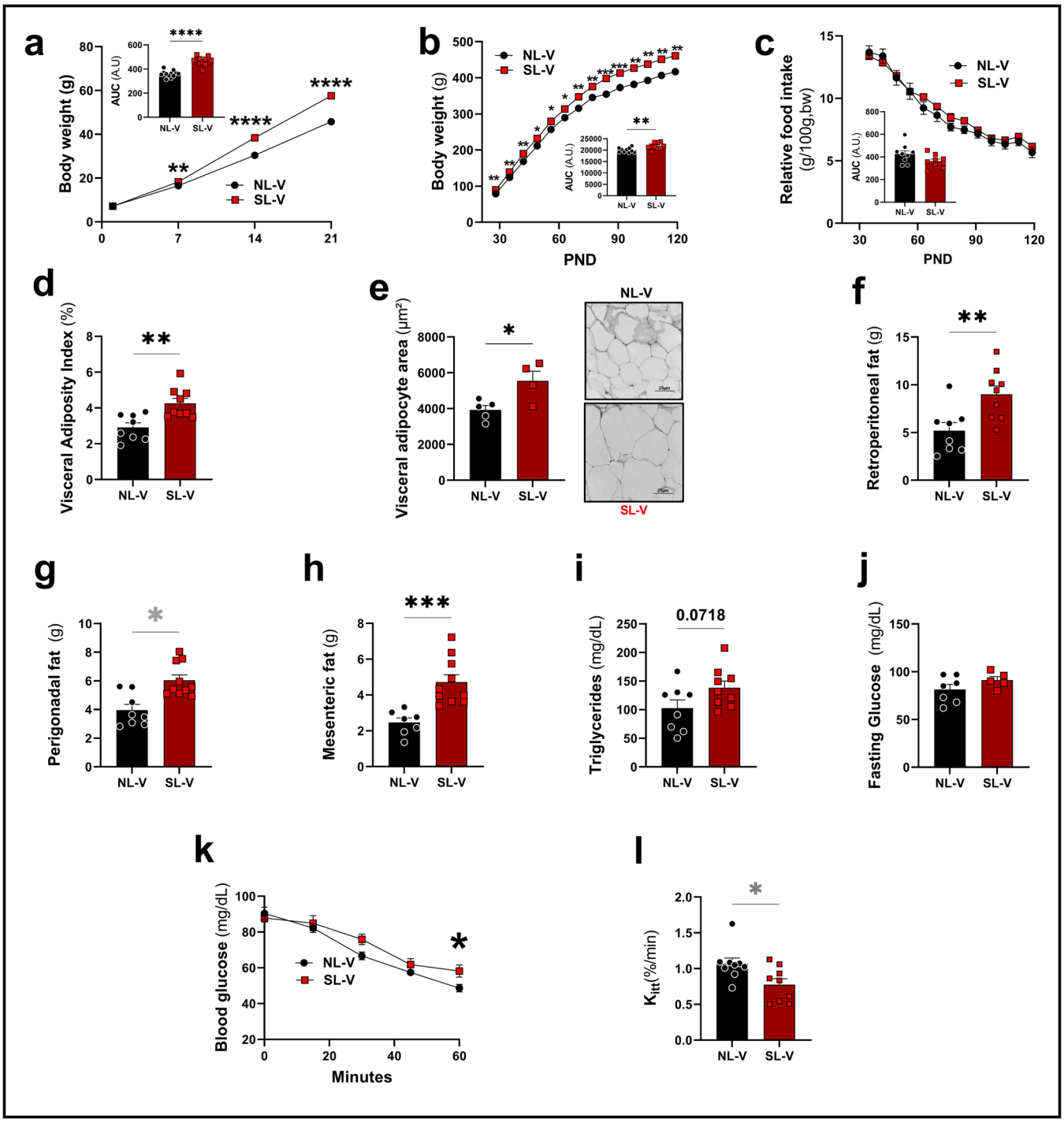

Fig. 2. Postnatal overfeeding leads to obesity and metabolic dysfunction at adulthood. (a) Bodyweight Evolution and Area Under the Curve during breastfeeding (AUC) (NL-V n = 10; SL-V n = 9). (b) Bodyweight Evolution and Area Under the Curve after weaning (AUC) (NL-V n = 10; SL-V n = 9). (c) Relative Food intake (NL-V n = 10; SL-V n = 9). (d) Visceral Adiposity (NL-V n = 8; SL-V n = 9). (e) Visceral adipocyte area (NL-V n = 5; SL-V n = 4). (f) Retroperitoneal fat depot (NL-V n = 8, SL-V n = 9). (g) Perigonadal fat depot (NL-V n = 8, SL-V n = 9). (h) Mesenteric fat depot (NL-V n = 7, SL-V n = 9). (i) Serum triglycerides (NL-V n = 7, SL-V n = 9). (j) Plasma Glucose (NL-V n = 7, SL-V n = 10). (k) Plasma glucose during Insulin Tolerance Test (NL-V n = 9, SL-V n = 9). (l) Decay of Glucose rate – kITT (NL-V n = 9, SL-V n = 9. Data are presented as mean ± SEM. To compare the experimental groups Student's *t*-test was used for parametric (in black) and Mann-Whitney for nonparametric data (in grey). *p < 0.05, **p < 0.01. ***p < 0.001.

indicate a defective oxidative metabolism in the liver of SL early in life.

Next, we explored whether AMPK-dependent oxidative capacity might be also impaired in two additional key metabolic organs: VAT and BAT. In the visceral adipose tissue, postnatal overfeeding leads to decreased tAMPK (Fig. 4f). On the BAT, we observed a trend towards decreased PPARα (Fig. 4j), and pAMPK (Fig. 4l). Together, SL animals presented decreased markers for oxidative metabolism, particularly, in the BAT (Figs. 4j and 4l). No difference was observed on total or phosphorylated ACL (Fig. 4h, i, m, n), a key enzyme that converts citrate to acetyl-CoA, linking carbohydrate metabolism to fatty acid synthesis. Therefore, we have hypothesized that postnatal overfeeding could program decreased BAT activity at adulthood.

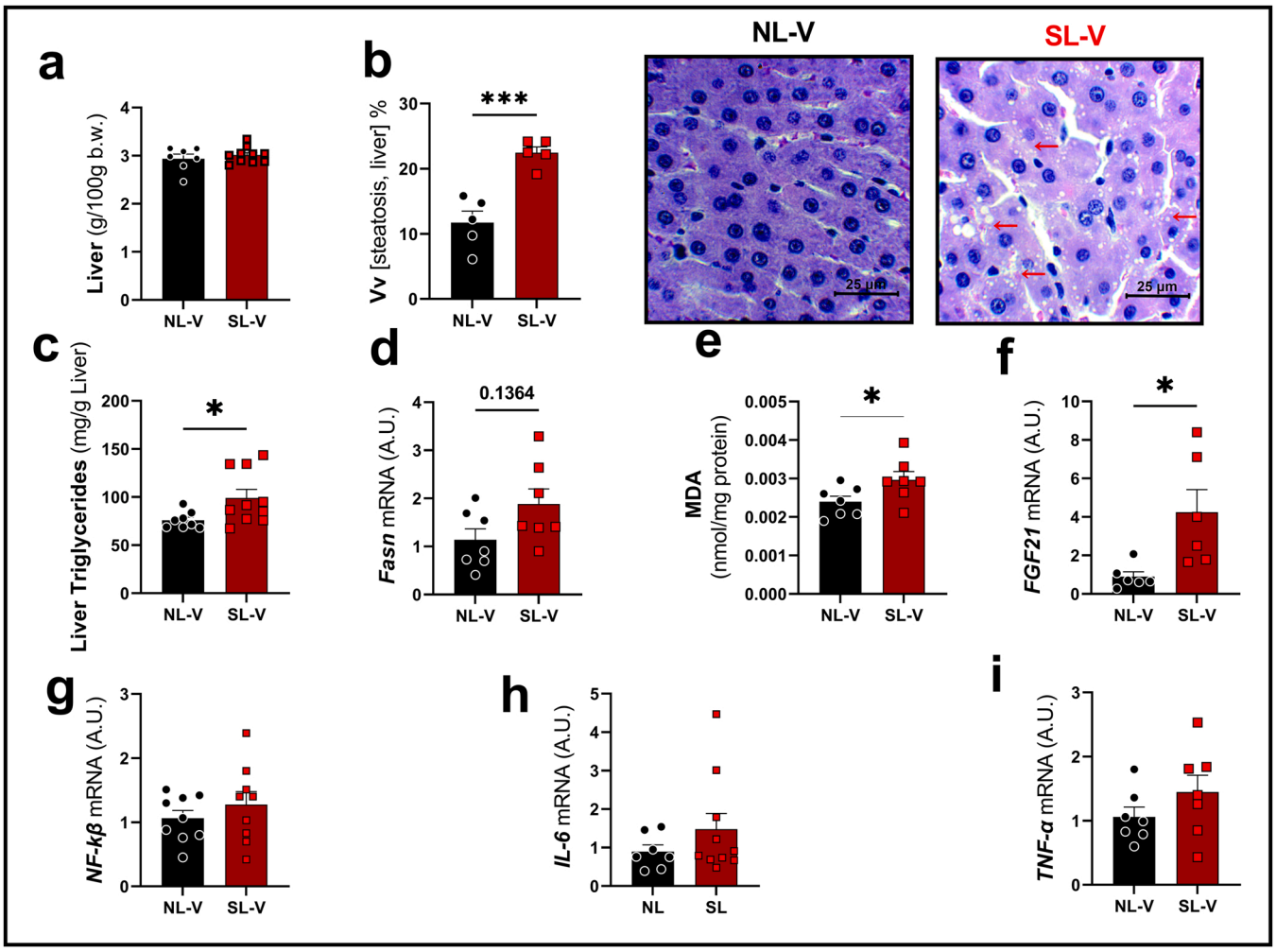

Fig. 3. Postnatal overfeeding causes liver lipid accumulation and increased *FGF21* expression. (a) Liver weight (NL-V n = 7; SL-V n = 10). (b) Liver steatosis score and representative images (NL-V n = 5; SL-V n = 5). (c) Liver triglycerides (NL-V n = 7; SL-V n = 10). (d) Liver *FASN* expression (NL-V n = 7; SL-V n = 7). (e) Liver lipid peroxidation -MDA (NL-V n = 7, SL-V n = 7). (f) Liver *FGF21* expression (NL-V n = 6, SL-V n = 5) (g) Liver *NFKβ* expression (NL-V n = 9, SL-V n = 10). (h) Liver IL-6 expression (NL-V n = 7, SL-V n = 10). (i) Liver *TNFα* expression (NL-V n = 7, SL-V n = 7). Data are presented as mean ± SEM. To compare the experimental groups Student's *t*-test was used for parametric (in black) and Mann-Whitney for nonparametric data (in grey). *p < 0.05, **p < 0.01. ***p < 0.001.

3.4. Childhood obesity induced by litter size reduction leads to decreased energy expenditure and reduced hypothalamic-BAT signaling

SL-V animals presented decreased AUC on energy expenditure for 24 hours (Fig. 5a) and decreased AUC on RQ (Fig. 5b). Also, childhood obesity led to decreased BAT sympathetic nerve activity (Fig. 5c, NL-V 19.31 ± 1.23 *vs* SL-V 11.77 ± 1.79 Spike/5 seconds, $p < 0.01$). We observed increased expression of *Fgf21* in the liver at adulthood, which is the main site of production for plasmatic levels [33]. FGF21 signaling in the hypothalamus leads to activation of HPA-axis and BAT sympathetic signaling. However, despite its increased expression, we observed decreased BAT sympathetic activity (Fig. 5c). When we evaluated FGF21 receptor, *Fgfr1*, we noted that its expression was decreased in the hypothalamus of obese animals (Fig. 5d, NL-V 1.05 ± 0.14 *vs* SL-V 0.46 ± 0.09 A.U., $p < 0.01$). No difference was observed in BAT weight, UCP-1 or lipid droplet area (Fig. 5e, f, g).

Together, our data supports that litter size reduction induced dysfunction on BAT autonomic sympathetic signaling, associated with decreased expression of FGF21 receptor in the hypothalamus. Considering the decreased PPARα activity observed in BAT and liver during early in life, and that postnatal activation of PPARα could be protective against obesity during adulthood, we hypothesized that increased PPARα activation, during lactation, induced by an agonist would be protective against the development of obesity and metabolic dysfunction in this model. To test the hypothesis, we treated SL pups with fenofibrate, a well characterized PPARα agonist, during lactation (Summarized in Fig. 1).

3.5. Fenofibrate treatment during lactation protects against the development of obesity and metabolic dysfunction induced by childhood obesity

First, we addressed any potential influence of PPARα activation early in life in normal litter. Hence, we treated a batch of controls with PPARα (NL-F, n = 6–10) similarly to the previous groups, however no effect was observed on the evaluated parameters when compared to NL-V. (Supplemental figure 2). In contrast, PPARα activation exclusively during lactation prevented excessive bodyweight gain in SL rats (Fig. 6a), without significant differences on food intake (Fig. 6b). Also, postnatal activation of PPARα prevented the development of visceral obesity (Fig. 6c), by decreasing the accumulation of retroperitoneal (Fig. 6d), perigonadal (Fig. 6e) and mesenteric fat pads (Fig. 6f). The previous modifications were accompanied with improvements on hypertriglyceridemia (Fig. 6g) and insulin sensitivity (Fig. 6h). Together, these results demonstrate that the administration of an PPARα agonist, fenofibrate, during lactation prevents the development of

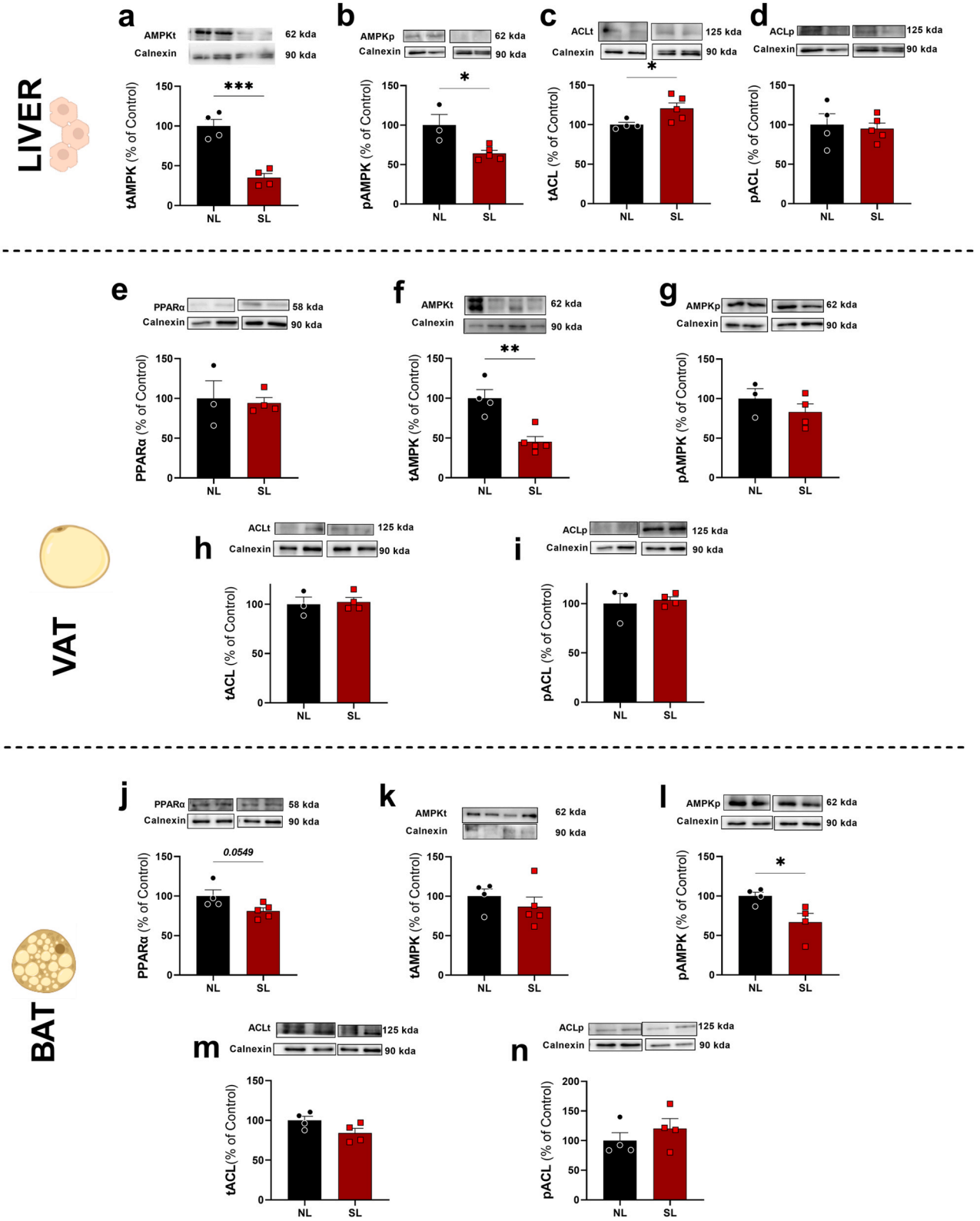

Fig. 4. Postnatal overfeeding increased BAT PPARα levels during lactation, as well as lower AMPK activity in liver and BAT early in life (PND14). (a) Liver total AMPK (NL-V n = 4; SL-V n = 4). (b) Liver phosphorylated Ampk (NL-V n = 3; SL-V n = 5). (c) Liver total ACL (NL-V n = 4; SL-V n = 5). (d) Liver phosphorylated ACL (NL-V n = 4; SL-V n = 5). (e) Visceral adipose tissue (VAT) PPARα (NL-V n = 3, SL-V n = 4). (f) VAT total AMPK (NL-V n = 4, SL-V n = 5). (g) VAT phosphorylated AMPK (NL-V n = 3, SL-V n = 4). (h) VAT total ACL (NL-V n = 3, SL-V n = 4). (i) VAT phosphorylated ACL (NL-V n = 3, SL-V n = 4). (j) Brown adipose tissue (BAT) PPARα (NL-V n = 4, SL-V n = 5). (i) BAT total AMPK (NL-V n = 4, SL-V n = 5). BAT phosphorylated AMPK (NL-V n = 4, SL-V n = 4). BAT total ACL (NL-V n = 4, SL-V n = 4). BAT phosphorylated ACL (NL-V n = 4, SL-V n = 4). Data are presented as mean ± SEM. To compare the experimental groups Student's *t*-test was used for parametric (in black) and Mann-Whitney for nonparametric data (in grey). *p < 0.05, ***p < 0.001.

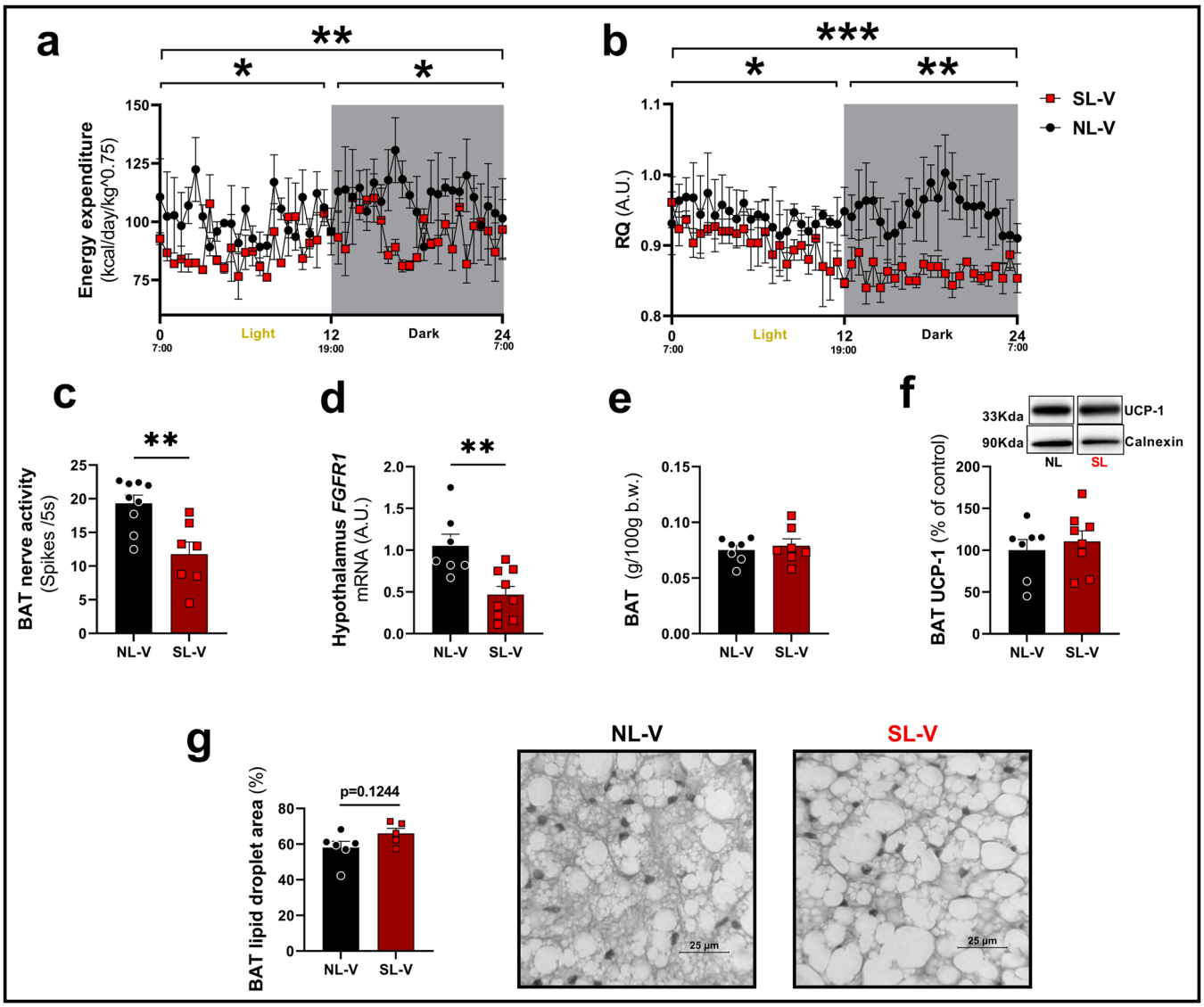

Fig. 5. Postnatal overfed animals shows decreased energy expenditure and reduced BAT sympathetic signaling. (a) 24 hours energy expenditure (NL-V n = 3; SL-V n = 3). (b) 24 hours respiratory quotient (NL-V n = 3; SL-V n = 3). (c) Brown adipose tissue (BAT) sympathetic nerve activity (NL-V n = 9; SL-V n = 7). (d) Hypothalamic *FGFR1* expression (NL-V n = 7; SL-V n = 9). (e) BAT-to-BW-ratio (NL-V n = 7; SL-V n = 7). (f) BAT UCP-1 (NL-V n = 7, SL-V n = 7). (g) %BAT lipid droplet area (NL-V n = 6, SL-V n = 5). Data are presented as mean ± SEM. To compare the experimental groups Student's *t*-test was used for parametric (in black) and Mann-Whitney for nonparametric data (in grey). *p < 0.05, ***p < 0.001.

obesity and metabolic dysfunction at adulthood in an animal model of childhood obesity.

3.6. *Fenofibrate treatment during lactation protects against the development of hepatic microvesicular steatosis induced by postnatal overfeeding*

Fenofibrate treatment during lactation decreased micro vesicular steatosis (Fig. 7a, SL-V 22.4 ± 0.914 *vs* SL-F 12.72 ± 2.493 %, p < 0.01) and triglycerides accumulation in the liver at adulthood (Fig. 7b, SL-V 99.13 ± 8.76 *vs* SL-F 73.42 ± 4.40 mg/g, p < 0.05). Despite the prevention of hepatic steatosis, we did not observe a significant reduction in oxidative stress markers or *Fgf21* expression (Fig. 7c and d). When oxidative stress marker MDA was correlated with *Fgf21* for all animals in pooled data, we observed a positive correlation between variables (Supplemental Figure 1k). Considering that oxidative stress and FGF21 levels were maintained, concomitantly with a prevention in the development of obesity, metabolic dysfunction and steatosis, we hypothesized that central signaling of FGF21 could be preserved.

3.7. *Fenofibrate treatment restored BAT sympathetic nervous system (SNS) activity and hypothalamic expression of FGFR1*

SL-F animals had increased BAT sympathetic innervation activity (Fig. 8a, SL-V 11.77 ± 1.79 *vs* SL-F 20.89 ± 2.87 spikes/5 seconds, p < 0.05), and hypothalamic *Fgfr1* expression (Fig. 8b, SL-V 0.46 ± 0.09 *vs* SL-F 1.00 ± 0.233 A.U., p < 0.05), indicating a restored response to FGF21, a known activator of BAT sympathetic innervation and activity [34]. It was observed a trend towards a diminished BAT lipid droplet area, an indicative of increased mobilization of stored triglycerides in the BAT (Fig. 8c, SL-V 65.99 ± 2.86 *vs* SL-F 58.1 ± 2.87 %, p = 0.08). No differences were observed on UCP-1 expression and total energy expenditure, RQ (Fig. 8d, e, f). Yet, a minor, nearly significant, improvement was observed in SL-F rats during the light cycle, which is the resting period for rodents and they rely on FFA oxidation.

4. Discussions

Here we found that administering fenofibrate, an PPARα agonist,

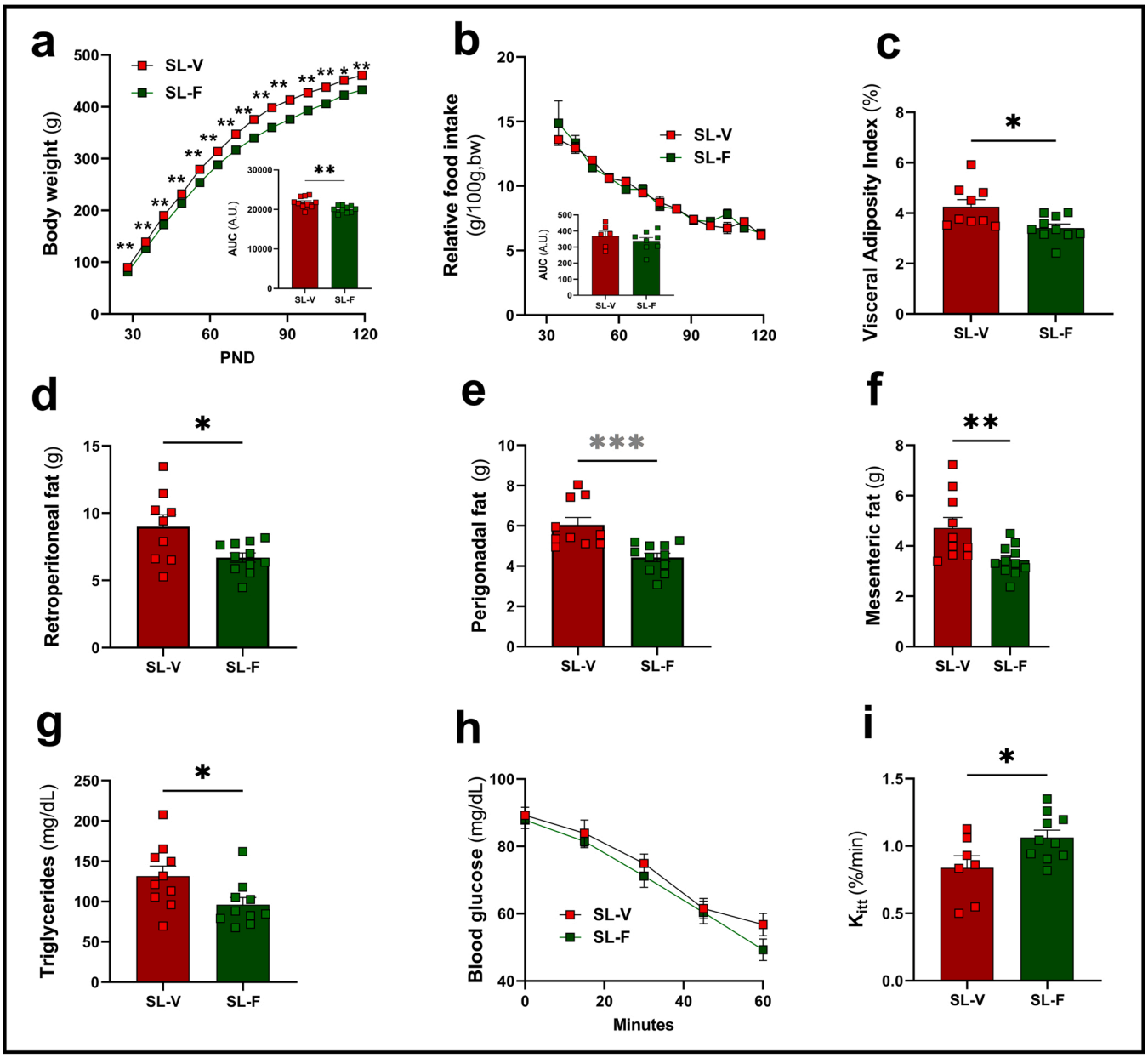

Fig. 6. Postnatal PPARα activation prevent obesity and metabolic dysfunction associated with postnatal overfeeding. (a) Bodyweight evolution and respective Area Under the Curve (AUC) (SL-V n = 10; SL-F n = 10). (b) Food intake evolution and AUC (SL-V n = 10; SL-F n = 10). (c) Visceral Adiposity (SL-V n = 9; SL-F n = 10). (d) Retroperitoneal fat depot (SL-V n = 9, SL-F n = 11). (e) Perigonadal fat depot (SL-V n = 10, SL-F n = 11). (f) Mesenteric fat depot (SL-V n = 10, SL-F n = 11). (g) Serum triglycerides (SL-V n = 9, SL-F n = 10). (h) Insulin Tolerance Test (SL-V n = 9, SL-F n = 9). (i) Decay of Glucose rate – K_{itt} (SL-V n = 9, SL-F n = 9. Data are presented as mean ± SEM. To compare the experimental groups Student's *t*-test was used for parametric (in black) and Mann-Whitney for nonparametric data (in grey). *p < 0.05, **p < 0.01. ***p < 0.001.

exclusively during lactation, was able to prevent the development of obesity, insulin resistance, liver microvesicular steatosis and sympathetic autonomic dysfunction associated with postnatal overfeeding. In the present study, we confirmed that postnatal overfeeding induced rapid weight gain at childhood, which persisted until adulthood, increased visceral obesity and insulin resistance, liver steatosis and increased oxidative stress, upregulation of *Fgfr1* expression and reduced BAT sympathetic nervous activity. Moreover, this model shows decreased BAT PPARα levels during lactation, as well as lower AMPK activity in liver and BAT at PND14. To the best of our knowledge, for the first time it was shown the dysregulation of the FGF21-FGFR1- SNS axis in postnatal overfed animals. Our data corroborate with previous studies showing that litter size reduction is a well-recognized animal model for childhood obesity, and later development of obesity and metabolic dysfunction [15,22,35].

Previous studies have shown that metabolic dysfunction in SL animals would be related to increased accumulation of diacylglycerol (DAG) within the liver [22]. DAG has been proposed as mechanism linking liver steatosis to oxidative stress and insulin resistance [36,37]. In the liver DAG is formed by a reaction catalyzed by the enzyme MOGAT1, which uses monoacylglycerol as a precursor, catalyzes the binding of an acyl group to the intermediary, forming DAG as product [36]. It was shown that high DAG levels activate PKC, promoting insulin resistance and formation of reactive oxygen species and local inflammation [36,37]. Despite not showing marked inflammation, postnatal overfeeding has been reported to lead to oxidative stress within the liver, which corroborates to our findings towards an increased trend for oxidative damage in this tissue [29,35]. In agreement with our findings,

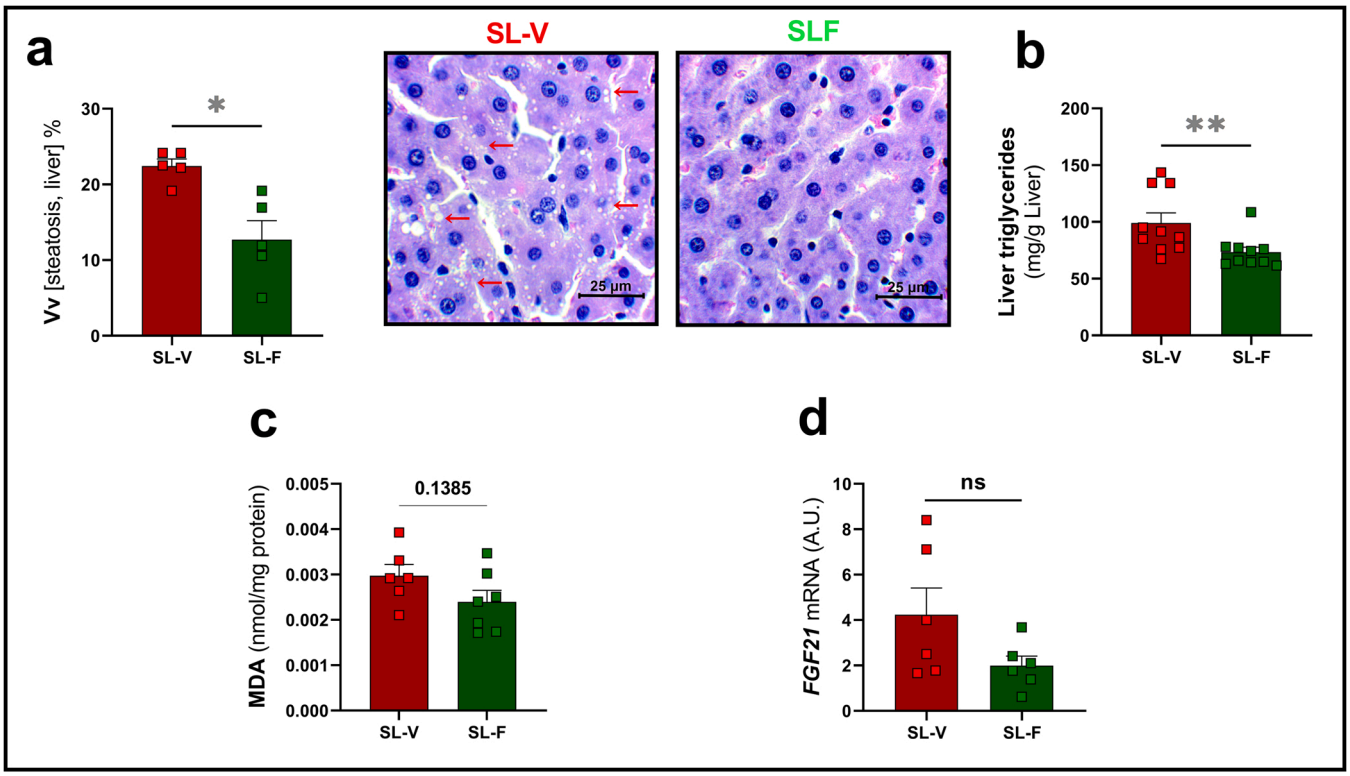

Fig. 7. Increased PPARα activation during lactation protects against the development of hepatic micro vesicular steatosis induced by postnatal overfeeding. (a) Liver steatosis score and representative images (SL-V n = 5; SL-F n = 5). (b) Liver triglycerides (SL-V n = 10; SL-F n = 10). (c) Liver lipid peroxidation marker - MDA (SL-V n = 6; SL-F n = 7). (d) Liver FGF21 expression (SL-V n = 6, SL-F n = 6). Data are presented as mean ± SEM. To compare the experimental groups Student's t test was used for parametric and Mann-Whitney for nonparametric data (in grey). *p < 0.05, **p < 0.01.

previous studies have shown that SL animals have increased expression of MOGAT1 and DAG during lactation, which persists until adulthood, mechanistically linking it to the development of hepatic steatosis and insulin resistance later in life[22]. Litter size reduction leads to alterations in breastmilk composition, markedly increased fat content which is accompanied by increased total milk intake by the pups, thus increasing fat intake during breastfeeding [38]. This increased flux of FFA from milk would increase hepatic triacylglycerol and DAG in the liver early in life [22]. The intracellular metabolism and oxidation, particularly in the liver is dependent of the transcription factor PPARα which is activated by lipids and which increases the expression of key enzymes in fatty acid oxidation, including *CPT1a*, *Acox1* and *Acadm* [17]. In humans breastfeeding was associated with increased PPARα expression in blood cells [39]. We have observed that postnatal fenofibrate administration prevented several disturbances related to lipid metabolism such as visceral obesity, dyslipidemia, liver steatosis and insulin resistance. Fenofibrate is a well-known PPARα agonist, which promotes lipid oxidation [17,40]. In Dahl salt-sensitive leptin receptor mutant rats (SSLepRmutant), an animal model of childhood/pre-pubertal obesity, it was observed that adulthood treatment with Gemfibrozil, a fibrate, at adulthood, was able improve hypertriglyceridemia, renal injury and kidney ectopic lipid accumulation [41,42]. Also, in a study with animal model of glycogen storage disease type Ia, which leads to severe hepatic steatosis during lactation, have shown that fenofibrate treatment during five days was able to significantly reduce hepatic steatosis by increasing mitochondrial fatty acid oxidation [21]. This effect was attributed to decreased levels of plasmatic acyl-carnitine and increased expression of genes related to lipid oxidation in the liver [21].

Therefore, despite not being addressed in our study, its plausible to hypothesize that fenofibrate may have prevented hepatic steatosis in the neonatal liver in a similar mechanism, which in turn would prevent lipid accumulation and insulin resistance at adulthood. Also, considering the beneficial effects of fenofibrate on diet induced obesity, we speculate that adulthood treatment with fenofibrate in small litter could also ameliorate obesity and metabolic dysfunction [43,44].

We have observed that SL-V animals had increased liver *Fgfr1* expression, which was prevented by PPARα activation early in life. Clinical and pre-clinical studies have shown that hepatic steatosis is accompanied by upregulation of *Fgf1* expression [45,46]. FGF21 is an hepatokine secreted mainly by the liver in stressful conditions, but also by other tissues, such as muscle, white adipose tissue, BAT and pancreas [33]. We have observed that postnatal overfeeding leads to steatosis and a trend towards oxidative damage, which in turn may be triggering *Fgf21* expression. Increased *Fgf21* expression has protective effects in metabolism, by promoting insulin sensitivity, VAT browning and BAT thermogenesis and fatty acid oxidation, while decreasing inflammation [47,48].

Similarly, to our findings, despite having increased *FGF21* expression, different models of obesity and hepatic steatosis are not protected against the development of obesity and insulin resistance [46]. FGF21 is a polypeptide that binds to a membrane receptor, FGFR1, and its co-receptor β-klotho. Therefore, it has been proposed that obesity and hepatic steatosis reassembles a FGF21 resistant state, where the hormone is not able to promote their effects within the cells [49,50]. Previous studies have shown that diet induced obesity leads to an FGF21 resistant state, by decreased expression of FGFR1 in peripheral tissues such as liver and VAT. However, in that model a causal relationship between FGF21 and obesity was not established since knockout for *Fgf21* did not develop increased obesity when fed a high-fat diet [49]. In postnatal overfed animals, increased metabolic and oxidative stress within the liver may be triggering increased *Fgf21* expression, which is prevented by PPARα activation. However, this may also be related to an FGF21 resistant state, since the expression of its receptor, FGFR1, is

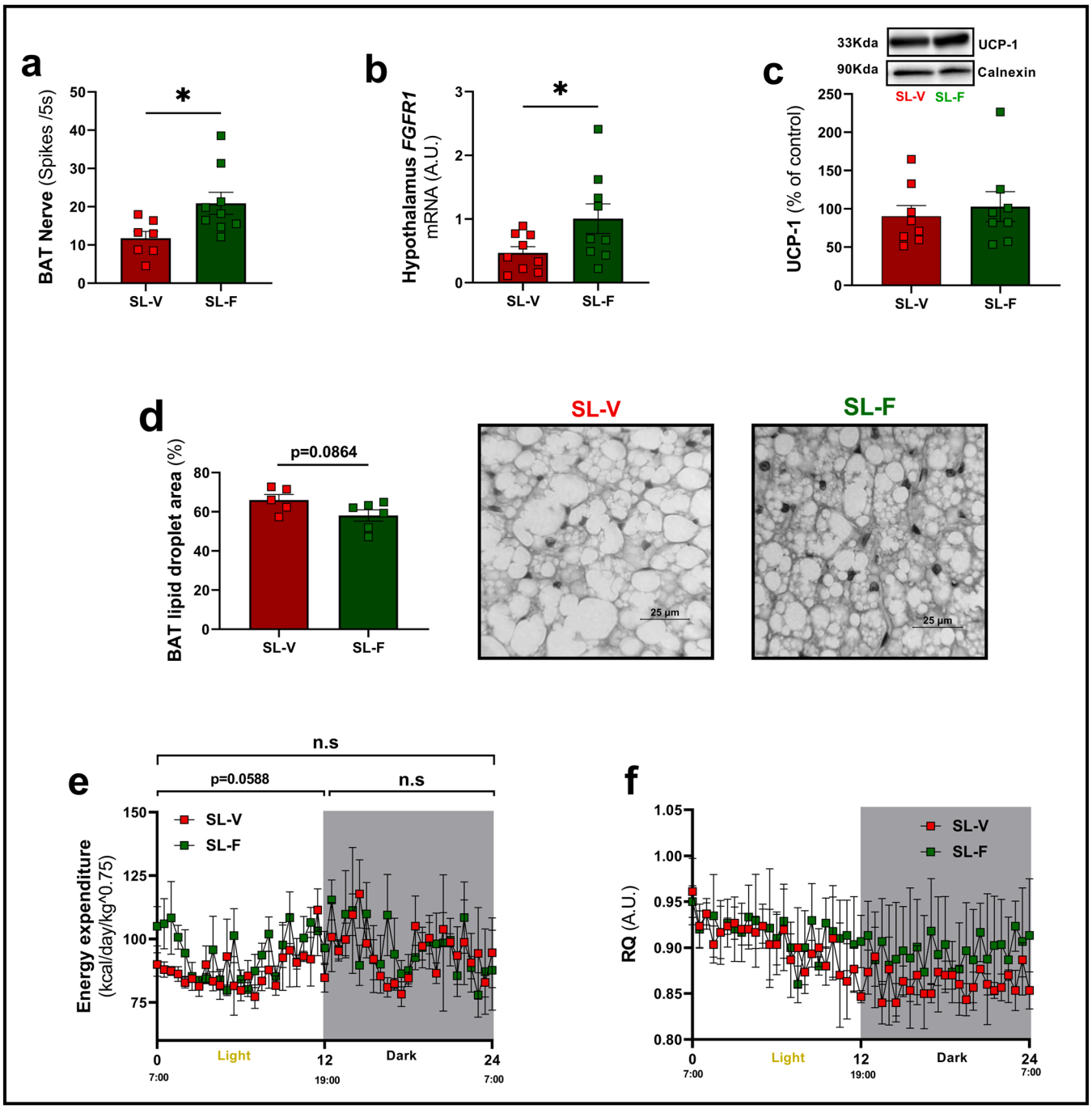

Fig. 8. Postnatal PPARα activation restored BAT sympathetic nervous system activity and hypothalamic expression of FGFR1. a) Brown adipose tissue (BAT) sympathetic nerve activity (SL-V n = 9; SL-F n = 9). (b) Hypothalamic *FGFR1* expression (SL-V n = 9; SL-F n = 9). (c) BAT UCP-1 (SL-V n = 8, SL-F n = 8). (d) %BAT lipid droplet area (SL-V n = 5, SL-F n = 5). (e) 24 hours energy expenditure (SL-V n = 3; SL-F n = 3). (f) 24 hours Respiratory quotient (SL-V n = 3; SL-F n = 3). Data are presented as mean ± SEM. To compare the experimental groups Student's *t*-test was used for parametric (in black) and Mann-Whitney for nonparametric data (in grey). *p < 0.05.

decreased in the hypothalamus.

Postnatal overfeeding leads to decreased sympathetic nervous activity which was accompanied by decreased *Fgfr1* expression in the hypothalamus. Beyond their peripheral effects, FGF21 was shown to have central effects in the hypothalamus, by promoting increased sympathetic nervous system activity and thermogenesis in BAT [34,51]. Regarding epigenetic programming, some studies have found a link between *Fgf21* expression and protection against the development of obesity and metabolic dysfunction later in life. Metabolic programming for disease during the critical phases of development have been proposed as an important factor for disease development later in life [52,53]. In fact, several studies explain these effects by alterations in gene expression modulated by epigenetic marks, such as DNA methylation, histone modification and mi-RNAs [54,55]. Maternal perinatal administration of an PPARα agonist, was able to confer protection against diet-induced obesity and metabolic dysfunction later in life, being observed a reduced degree of repressive methylation on *Fgf21* promoter gene, which persisted until adulthood [56].

In our study an increased PPARα activity, induced by direct administration of an agonist to the pup was able to prevent the long-term

metabolic dysfunction induced by postnatal overfeeding, despite also downregulating *Fgf21* expression, showing that the protective effect may be related to a different mechanism. An animal study has found that delayed weaning was able to confer this protection by increasing Fgf21 levels in the offspring when fed a HFD [57]. Also, it was found that the hypothalamic signaling via FGF21-*d2r*-expressing GABAergic neurons in the hypothalamus, was necessary to the observed effect [57]. We have observed that SL animals show decreased sympathetic nervous activity which was accompanied by decreased *Fgf21* expression in the hypothalamus. Despite the increased *Fgf21* expression in the liver, which in turn would be associated with increased sympathetic activity, SL-V animals show decreased BAT sympathetic activity, which could be caused by a central resistance to FGF21 effects.

Our study has some limitations since we were not able to measure the effect of fenofibrate treatment on liver DAG levels, or the expression of FGFR1 in peripheral tissues such as BAT, VAT and liver. Central FGF21 resistance could also be tested through an intracerebroventricular injection of an analogue. Even with some limitations, to the best of our knowledge, for the first time it was shown the dysregulation of the FGF21-FGFR1-sympathetic axis in an animal model of childhood obesity. Also, we provide preclinical evidence that adipose tissue and liver associated metabolic dysfunction, induced by childhood obesity at adulthood, could be prevented by early in life treatment with a PPARα agonist.

5. Conclusions

Fenofibrate treatment during lactation prevented visceral obesity, BAT autonomic sympathetic hypoactivity, liver microvesicular steatosis, and associated metabolic dysfunction, long-term programed in an animal model of childhood obesity. These effects could be mediated through activation of PPARα during early life. Despite the beneficial effects observed in this study, the translational implications of this treatment for humans must be further investigated, considering safety concerns related to fibrate use in neonates or individuals with compromised hepatic or renal function.

Authors contribution

LPJS, SRR, ALMA, NCL, AA, MDFJ, MNCP, SP, GDG, VMM, LFB, DS and FCFS performed the experiments for animal maintenance and sample collection. LPJS and ALMA performed the histological analysis. LPJS, JCJC, NCL, DS and PM performed the molecular biology analyzes. FCFS and JBG performed the oxidative stress activity analyzes. LPJS, DLA and PCFM, conceptualized the hypothesis and experimental design. LPJS, JCJC and DLA analyzed and interpreted the data. All authors have reviewed contributed to the writing and approved the submitted version of the paper.

CRediT authorship contribution statement

Barbosa Letícia Ferreira: Writing – review & editing, Methodology, Investigation. **de Freitas Mathias Paulo Cezar:** Writing – review & editing, Visualization, Supervision, Funding acquisition. **Sousa Diana:** Writing – review & editing, Methodology, Investigation. **dos Santos Flávia Caroline Farias:** Writing – review & editing, Methodology, Investigation. **Gonçalves Gessica Dutra:** Writing – review & editing, Methodology, Investigation. **Jiménez-Chillarón Josep C:** Writing – review & editing, Visualization, Formal analysis, Data curation. **Moreira Veridiana Mota:** Writing – review & editing, Methodology, Investigation. **Almeida Douglas Lopes:** Writing – review & editing, Visualization, Supervision, Formal analysis. **Chimirri Peres Maria Natália:** Writing – review & editing, Methodology, Investigation. **Comar Jurandir Fernando:** Writing – review & editing, Methodology, Investigation. **Piovan Silvano:** Writing – review & editing, Methodology, Investigation. **Gomes Rodrigo Mello:** Writing – review & editing, Methodology, Investigation. **Graceli Jones Bernardes:** Writing – review & editing, Methodology, Investigation. **Assakawa Ana Letícia Manso:** Writing – review & editing, Methodology, Investigation. **Lucredi Naiara Cristina:** Writing – review & editing, Methodology, Investigation. **Matafome Paulo:** Writing – review & editing, Supervision, Methodology, Investigation. **Amaro Andreia:** Writing – review & editing, Methodology, Investigation. **Jacinto Saavedra Lucas Paulo:** Writing – review & editing, Writing – original draft, Project administration, Methodology, Investigation, Formal analysis, Data curation, Conceptualization. **Ferreira-Junior Marcos Divino:** Writing – review & editing, Methodology, Investigation. **Raposo Scarlett Rodrigues:** Writing – review & editing, Methodology, Investigation.

Declaration of Competing Interest

The authors declare that they have no known competing financial interests or personal relationships that could have appeared to influence the work reported in this paper.

Acknowledgements

We would like acknowledge technicians and students from the Experimental Laboratory of DOHaD (LexDOHaD), for their technical support. Also, we would like to acknowledge Dr. Maria Aparecida Fernandez for the use of her laboratory facilities, and Dr. Carlos Henrique Grossi Sponton for valuable insights during thesis defensis.

We would like to thank the Brazilian Funding Agencies: Conselho Nacional de Desenvolvimento Científico e Tecnológico (CNPq); Coordenação de Aperfeiçoamento Pessoal de Nível Superior (CAPES); JBS, "Fazer o bem faz bem"; São Paulo Research Foundation (FAPESP) [grant number 2021/04664–7 - fellowship number 2023/13857–9. All authors have read the journal's authorship agreement, and the manuscript has been reviewed and approved by all authors. The authors declare that they have no competing interests.

Appendix A. Supporting information

Supplementary data associated with this article can be found in the online version at doi:10.1016/j.biopha.2025.118166.

References

[1] WHO, 2024, Obesity and Overweight: Fact Sheet⟨https://www.who.int/news-room/fact-sheets/detail/obesity-and-overweight⟩.
[2] WHO, 2024, Diabetes: Fact Sheet⟨https://www.who.int/news-room/fact-sheets/detail/diabetes⟩.
[3] WHO, 2021, Cardiovascular Diseases (CVDs): Fact Sheet⟨https://www.who.int/news-room/fact-sheets/detail/cardiovascular-diseases-(cvds)⟩.
[4] WHO, 2021, Infant and Young Child Feeding⟨https://www.who.int/news-room/fact-sheets/detail/infant-and-young-child-feeding⟩.
[5] C. Pico, F. Reis, C. Egas, P. Mathias, P. Matafome, Lactation as a programming window for metabolic syndrome, Eur. J. Clin. Invest. 51 (5) (2021) e13482.
[6] P.C. Lisboa, R.A. Miranda, L.L. Souza, E.G. Moura, Can breastfeeding affect the rest of our life? Neuropharmacology 200 (2021) 108821.
[7] C.G. Victora, R. Bahl, A.J. Barros, G.V. Franca, S. Horton, J. Krasevec, S. Murch, M. J. Sankar, N. Walker, N.C. Rollins, G. Lancet, Breastfeeding Series, Breastfeeding in the 21st century: epidemiology, mechanisms, and lifelong effect, Lancet 387 (10017) (2016) 475–490.
[8] I.P. Martins, J.C. de Oliveira, A. Pavanello, C.C.I. Matiusso, C. Previate, L.P. Tofolo, T.A. Ribeiro, C.C. da Silva Franco, R.A. Miranda, K.V. Prates, V.S. Alves, F. A. Francisco, A.M.P. de Moraes, P.C. de Freitas Mathias, A. Malta, Protein-restriction diet during the suckling phase programs rat metabolism against obesity and insulin resistance exacerbation induced by a high-fat diet in adulthood, J. Nutr. Biochem. 57 (2018) 153–161.
[9] L. Song, J. Cui, N. Wang, R. Wang, J. Yan, B. Sun, Maternal exercise during gestation and lactation decreases high-fat diet preference by altering central reward system gene expression in adult female offspring from high-fat fed dams, Behav. Brain Res. 390 (2020) 112660.
[10] F.A. Francisco, L.P.J. Saavedra, M.D.F. Junior, C. Barra, P. Matafome, P.C. F. Mathias, R.M. Gomes, Early AGEing and metabolic diseases: is perinatal exposure to glycotoxins programming for adult-life metabolic syndrome? Nutr. Rev. 79 (1) (2021) 13–24.

[11] R.A. Miranda, E. Gaspar de Moura, P.C. Lisboa, Tobacco smoking during breastfeeding increases the risk of developing metabolic syndrome in adulthood: Lessons from experimental models, Food Chem. Toxicol. 144 (2020) 111623.
[12] L.F. Grilo, C. Tocantins, M.S. Diniz, R.M. Gomes, P.J. Oliveira, P. Matafome, S. P. Pereira, Metabolic disease programming: from mitochondria to epigenetics, glucocorticoid signalling and beyond, Eur. J. Clin. Invest. 51 (10) (2021) e13625.
[13] L.L. Souza, E.G. Moura, P.C. Lisboa, Litter size reduction as a model of overfeeding during lactation and its consequences for the development of metabolic diseases in the offspring, Nutrients 14 (10) (2022).
[14] M. Parra-Vargas, S.G. Bouret, J.C. Bruning, E.G. de Moura, T. Garland Jr., P. C. Lisboa, S.E. Ozanne, M.E. Patti, A. Plagemann, J.R. Speakman, M. Tena-Sempere, C. Vergely, L.M. Zeltser, J.C. Jimenez-Chillaron, The long-lasting shadow of litter size in rodents: litter size is an underreported variable that strongly determines adult physiology, Mol. Metab. 71 (2023) 101707.
[15] M. Parra-Vargas, M. Ramon-Krauel, C. Lerin, J.C. Jimenez-Chillaron, Size does matter: litter size strongly determines adult metabolism in rodents, Cell Metab. 32 (3) (2020) 334–340.
[16] M.D.F. Junior, K.V.N. Cavalcante, L.A. Ferreira, P.R. Lopes, C.N.R. Pontes, A.S. M. Bessa, A.R. Neves, F.A. Francisco, G.R. Pedrino, C.H. Xavier, P.C.F. Mathias, C. H. Castro, R.M. Gomes, Postnatal early overfeeding induces cardiovascular dysfunction by oxidative stress in adult male Wistar rats, Life Sci. 226 (2019) 173–184.
[17] M. Rakhshandehroo, B. Knoch, M. Muller, S. Kersten, Peroxisome proliferator-activated receptor alpha target genes, PPAR Res. 2010 (2010).
[18] K. Hashimoto, Y. Ogawa, Epigenetic switching and neonatal nutritional environment, Adv. Exp. Med Biol. 1012 (2018) 19–25.
[19] T. Ehara, Y. Kamei, X. Yuan, M. Takahashi, S. Kanai, E. Tamura, K. Tsujimoto, T. Tamiya, Y. Nakagawa, H. Shimano, T. Takai-Igarashi, I. Hatada, T. Suganami, K. Hashimoto, Y. Ogawa, Ligand-activated PPARalpha-dependent DNA demethylation regulates the fatty acid beta-oxidation genes in the postnatal liver, Diabetes 64 (3) (2015) 775–784.
[20] D. Abdelmoneim, M. El-Adl, G. El-Sayed, E.S. El-Sherbini, Protective effect of fenofibrate against high-fat-high-fructose diet induced non-obese NAFLD in rats, Fundam. Clin. Pharmacol. 35 (2) (2021) 379–388.
[21] Z.A. Yavarow, H.R. Kang, L.R. Waskowicz, B.H. Bay, S.P. Young, P.M. Yen, D. D. Koeberl, Fenofibrate rapidly decreases hepatic lipid and glycogen storage in neonatal mice with glycogen storage disease type Ia, Hum. Mol. Genet. 29 (2) (2020) 286–294.
[22] M. Ramon-Krauel, T. Pentinat, V.W. Bloks, J. Cebria, S. Ribo, R. Perez-Wienese, M. Vila, I. Palacios-Marin, A. Fernandez-Perez, M. Vallejo, N. Tellez, M. A. Rodriguez, O. Yanes, C. Lerin, R. Diaz, T. Plosch, U.J.F. Tietge, J.C. Jimenez-Chillaron, Epigenetic programming at the Mogat1 locus may link neonatal overnutrition with long-term hepatic steatosis and insulin resistance, FASEB J. (2018) fj201700717RR.
[23] D.L. Almeida, V.M. Moreira, L.E. Cardoso, M.D.F. Junior, A. Pavanelo, T.A. Ribeiro, C.C. da Silva Franco, L.P. Tofolo, M.N.C. Peres, M.V.G. Ribeiro, A.R.O. Ferreira, R. M. Gomes, R.A. Miranda, I.H. Trevenzoli, J.A. Armitage, K. Palma-Rigo, P.C. de Freitas Mathias, Lean in one way, in obesity another: effects of moderate exercise in brown adipose tissue of early overfed male Wistar rats, Int. J. Obes. (Lond.) 46 (1) (2022) 137–143.
[24] I.P. Martins, R. Vargas, L.P.J. Saavedra, S. Rickli, C.C.I. Matiusso, A. Pavanello, L. Casagrande, M.J. Pastre, J.B. Oliveira, A.M. de Almeida, A.C.H. de Souza, J.C. de Oliveira, A. Malta, P.C.F. Mathias, Protein-caloric restriction induced HPA axis activation and altered the milk composition imprint metabolism of weaned rat offspring, Nutrition 108 (2022) 111945.
[25] K. Valerio Prates, T.A. Ribeiro, A. Pavanello, L.P. Jacinto Saavedra, V.M. Moreira, S. da Silva Silveira, I.P. Martins, F.A. Francisco, M.D. Ferreira Junior, V.S. Alves, L. P. Tofolo, C. Previate, C.C. da Silva Franco, R.M. Gomes, K. Palma-Rigo, A. Malta, P.C. de Freitas Mathias, Potential attenuation of early-life overfeeding-induced metabolic dysfunction by chronic maternal acetylcholinesterase inhibitor exposure, Toxicology 425 (2019) 152250.
[26] K.J. Livak, T.D. Schmittgen, Analysis of relative gene expression data using real-time quantitative PCR and the 2(-Delta Delta C(T)) Method, Methods 25 (4) (2001) 402–408.
[27] J. Folch, M. Lees, G.H.Sloane Stanley, A simple method for the isolation and purification of total lipides from animal tissues, J. Biol. Chem. 226 (1) (1957) 497–509.
[28] M. Catta-Preta, L.S. Mendonca, J. Fraulob-Aquino, M.B. Aguila, C.A. Mandarim-de-Lacerda, A critical analysis of three quantitative methods of assessment of hepatic steatosis in liver biopsies, Virchows Arch. 459 (5) (2011) 477–485.
[29] E.P. Conceicao, E.G. Moura, P.N. Soares, X.X. Ai, M.S. Figueiredo, E. Oliveira, P. C. Lisboa, High calcium diet improves the liver oxidative stress and microsteatosis in adult obese rats that were overfed during lactation, Food Chem. Toxicol. 92 (2016) 245–255.
[30] J.W.R.Daqing Piao, G.Reed Holyoak, Corey R. Wall, Nigar Sultana, Jill K. Murray, Kenneth E. Bartels†, n vivopercutaneous reflectance spectroscopyof fatty liver development in rats suggests thatthe elevation of the scattering power is an earlyindicator of hepatic steatosis, J. Innov. Opt. Health Sci. 11 (4) (2018) 19.
[31] A.B.Suvitha Syam, Najihah Mohd Hashim, Mostafa Ghaderian, Yahya Hasan Hobani, Anwar Makeen, Siddig Ibrahim Abdelwahab, Syam Mohan, β-Mangostin suppresses LA-7 cells proliferation in vitro and in vivo: involvement of antioxidant enzyme modulation; suppression of matrix metalloproteinase and α6β4 integrin signalling pathways, J. Funct. Foods 22 (2016) 504–517.
[32] P.L. Podratz, E. Merlo, J.F.P. de Araujo, J.G.M. Ayub, A.F.Z. Pereira, L.C. Freitas-Lima, M.B. da Costa, L. Miranda-Alves, S.G.S. Cassa, M. Carneiro, G. Fillmann, J. B. Graceli, Disruption of fertility, placenta, pregnancy outcome, and multigenerational inheritance of hepatic steatosis by organotin exposure from contaminated seafood in rats, Sci. Total Environ. 723 (2020) 138000.
[33] J.E. Lewis, F.J.P. Ebling, R.J. Samms, K. Tsintzas, Going back to the biology of FGF21: new insights, Trends Endocrinol. Metab. 30 (8) (2019) 491–504.
[34] B.M. Owen, X. Ding, D.A. Morgan, K.C. Coate, A.L. Bookout, K. Rahmouni, S. A. Kliewer, D.J. Mangelsdorf, FGF21 acts centrally to induce sympathetic nerve activity, energy expenditure, and weight loss, Cell Metab. 20 (4) (2014) 670–677.
[35] E.P. Conceicao, J.G. Franco, E. Oliveira, A.C. Resende, T.A. Amaral, N. Peixoto-Silva, M.C. Passos, E.G. Moura, P.C. Lisboa, Oxidative stress programming in a rat model of postnatal early overnutrition–role of insulin resistance, J. Nutr. Biochem. 24 (1) (2013) 81–87.
[36] D.M. Erion, G.I. Shulman, Diacylglycerol-mediated insulin resistance, Nat. Med. 16 (4) (2010) 400–402.
[37] K.W. Ter Horst, P.W. Gilijamse, R.I. Versteeg, M.T. Ackermans, A.J. Nederveen, S. E. la Fleur, J.A. Romijn, M. Nieuwdorp, D. Zhang, V.T. Samuel, D.F. Vatner, K. F. Petersen, G.I. Shulman, M.J. Serlie, Hepatic diacylglycerol-associated protein kinase cepsilon translocation links hepatic steatosis to hepatic insulin resistance in humans, Cell Rep. 19 (10) (2017) 1997–2004.
[38] D.X.S. João Lucas P Xavier 1, Catherine C. Pontes 1, Paulo Roberto Ribeiro 1, Maiara M. Cordeiro 1, Jessica A. Marcondes 1, Felipe O. Mendonça 1, Makcine T. da Silva 1, Fabio B. de Oliveira 1, Gilson C.N. Franco 1, Sabrina Grassiolli 2, Litter size reduction induces metabolic and histological adjustments in dams throughout lactation with early effects on offspring, An. da Acad. Bras. De. Ciências 91 (2019).
[39] S. Cheshmeh, S.M. Nachvak, N. Rezvani, A. Saber, Effects of breastfeeding and formula feeding on the expression level of FTO, CPT1A and PPAR-alpha genes in healthy infants, Diabetes Metab. Syndr. Obes. 13 (2020) 2227–2237.
[40] T.L. Rachid, A. Penna-de-Carvalho, I. Bringhenti, M.B. Aguila, C.A. Mandarim-de-Lacerda, V. Souza-Mello, PPAR-alpha agonist elicits metabolically active brown adipocytes and weight loss in diet-induced obese mice, Cell Biochem Funct. 33 (4) (2015) 249–256.
[41] B. Poudel, C.A. Shields, U.S. Ekperikpe, A.K. Brown, O.K. Travis, J.C. Maury, S. Fitzgerald, S.V. Smith, D.C. Cornelius, J.M. Williams, The SS(LepR) mutant rat represents a novel model to study obesity-induced renal injury before puberty, Am. J. Physiol. Regul. Integr. Comp. Physiol. 322 (4) (2022) R299–R308.
[42] C.A. Shields, B. Poudel, K.C. McPherson, A.K. Brown, U.S. Ekperikpe, E. Browning, L. Sutton, D.C. Cornelius, J.M. Williams, Treatment With Gemfibrozil Prevents the Progression of Chronic Kidney Disease in Obese Dahl Salt-Sensitive Rats, Front Physiol. 11 (2020) 566403.
[43] T.L. Rachid, A. Penna-de-Carvalho, I. Bringhenti, M.B. Aguila, C.A. Mandarim-de-Lacerda, V. Souza-Mello, Fenofibrate (PPARalpha agonist) induces beige cell formation in subcutaneous white adipose tissue from diet-induced male obese mice, Mol. Cell Endocrinol. 402 (2015) 86–94.
[44] J. Yoo, I.K. Jeong, K.J. Ahn, H.Y. Chung, Y.C. Hwang, Fenofibrate, a PPARalpha agonist, reduces hepatic fat accumulation through the upregulation of TFEB-mediated lipophagy, Metabolism 120 (2021) 154798.
[45] M.M. Richter, I.M. Kemp, S. Heeboll, M. Winther-Sorensen, S.A.S. Kjeldsen, N. J. Jensen, J.D. Nybing, F.H. Linden, E. Hogh-Schmidt, M.P. Boesen, S. Madsbad, F. V. Schiodt, K. Norgaard, S. Schmidt, L.L. Gluud, S.B. Haugaard, J.J. Holst, S. Nielsen, J. Rungby, N.J. Wewer Albrechtsen, Glucagon augments the secretion of FGF21 and GDF15 in MASLD by indirect mechanisms, Metabolism (2024) 155915.
[46] B. Tucker, H. Li, X. Long, K.A. Rye, K.L. Ong, Fibroblast growth factor 21 in non-alcoholic fatty liver disease, Metabolism 101 (2019) 153994.
[47] K.H. Kim, M.S. Lee, FGF21 as a mediator of adaptive responses to stress and metabolic benefits of anti-diabetic drugs, J. Endocrinol. 226 (1) (2015) R1–R16.
[48] L. Geng, K.S.L. Lam, A. Xu, The therapeutic potential of FGF21 in metabolic diseases: from bench to clinic, Nat. Rev. Endocrinol. 16 (11) (2020) 654–667.
[49] F.M. Fisher, P.C. Chui, P.J. Antonellis, H.A. Bina, A. Kharitonenkov, J.S. Flier, E. Maratos-Flier, Obesity is a fibroblast growth factor 21 (FGF21)-resistant state, Diabetes 59 (11) (2010) 2781–2789.
[50] Q. Liu, S. Wang, M. Wei, X. Huang, Y. Cheng, Y. Shao, P. Xia, M. Zhong, S. Liu, G. Zhang, S. Hu, Improved FGF21 sensitivity and restored FGF21 signaling pathway in high-fat diet/streptozotocin-induced diabetic rats after duodenal-jejunal bypass and sleeve gastrectomy, Front Endocrinol. (Lausanne) 10 (2019) 566.
[51] N. Douris, D.M. Stevanovic, F.M. Fisher, T.I. Cisu, M.J. Chee, N.L. Nguyen, E. Zarebidaki, A.C. Adams, A. Kharitonenkov, J.S. Flier, T.J. Bartness, E. Maratos-Flier, Central fibroblast growth factor 21 browns white fat via sympathetic action in male mice, Endocrinology 156 (7) (2015) 2470–2481.
[52] D.L. Almeida, A. Pavanello, L.P. Saavedra, T.S. Pereira, M.A.A. de Castro-Prado, P. C. de Freitas Mathias, Environmental monitoring and the developmental origins of health and disease, J. Dev. Orig. Health Dis. 10 (6) (2019) 608–615.
[53] C.N. Hsu, C.Y. Hou, W.H. Hsu, Y.L. Tain, Early-life origins of metabolic syndrome: mechanisms and preventive aspects, Int J. Mol. Sci. 22 (21) (2021).
[54] P.M.C.Keith M. Godfrey, Karen A. Lillycrop, Development, epigenetics and metabolic programming, Nestle Nutr. Inst. Workshop Ser. 85 (2016) 71–80.
[55] P.G.A.M. Hanson, Developmental and epigenetic pathways to obesity: ⦸an evolutionary-developmental perspective, Int. J. Obes. 32 (2008).
[56] X. Yuan, K. Tsujimoto, K. Hashimoto, K. Kawahori, N. Hanzawa, M. Hamaguchi, T. Seki, M. Nawa, T. Ehara, Y. Kitamura, I. Hatada, M. Konishi, N. Itoh, Y. Nakagawa, H. Shimano, T. Takai-Igarashi, Y. Kamei, Y. Ogawa, Epigenetic modulation of Fgf21 in the perinatal mouse liver ameliorates diet-induced obesity in adulthood, Nat. Commun. 9 (1) (2018) 636.
[57] V. Pena-Leon, C. Folgueira, S. Barja-Fernandez, R. Perez-Lois, N. Da Silva Lima, M. Martin, V. Heras, S. Martinez-Martinez, P. Valero, C. Iglesias, M. Duquenne, O. Al-Massadi, D. Beiroa, Y. Souto, M. Fidalgo, R. Sowmyalakshmi, D. Guallar,

J. Cunarro, C. Castelao, A. Senra, P. Gonzalez-Saenz, R. Vazquez-Cobela, R. Leis, G. Sabio, H. Mueller-Fielitz, M. Schwaninger, M. Lopez, S. Tovar, F.F. Casanueva, E. Valjent, C. Dieguez, V. Prevot, R. Nogueiras, L.M. Seoane, Prolonged breastfeeding protects from obesity by hypothalamic action of hepatic FGF21, Nat. Metab. 4 (7) (2022) 901–917.